5-2024

Population Pharmacokinetic Analysis of Atomoxetine and its Metabolites in Children and Adolescents with Attention-Deficit/ Hyperactivity Disorder.

Shen Cheng

Mahmoud Al-Kofahi

J Steven Leeder
Children's Mercy Hospital

Jacob T. Brown

Recommended Citation

Cheng S, Al-Kofahi M, Leeder JS, Brown JT. Population Pharmacokinetic Analysis of Atomoxetine and its Metabolites in Children and Adolescents with Attention-Deficit/Hyperactivity Disorder. Clin Pharmacol Ther. 2024;115(5):1033-1043. doi:10.1002/cpt.3155

Population Pharmacokinetic Analysis of Atomoxetine and its Metabolites in Children and Adolescents with Attention-Deficit/Hyperactivity Disorder

Shen Cheng[1,4], Mahmoud Al-Kofahi[1,5], J. Steven Leeder[2] and Jacob T. Brown[3,*]

Atomoxetine (ATX) is a non-stimulant used to treat attention-deficit/hyperactivity disorder (ADHD) and systemic exposure is highly variable due to polymorphic cytochrome P450 2D6 (CYP2D6) activity. The objective of this study was to characterize the time course of ATX and metabolites (4-hydroxyatomoxetine (4-OH); *N*-desmethylatomoxetine (NDA); and 2-carboxymethylatomoxetine (2-COOH)) exposure following oral ATX dosing in children with ADHD to support individualized dosing. A nonlinear mixed-effect modeling approach was used to analyze ATX, 4-OH, and NDA plasma and urine, and 2-COOH urine profiles obtained over 24–72 hours from children with ADHD ($n = 23$) following a single oral ATX dose. Demographics and CYP2D6 activity score (AS) were evaluated as covariates. Simulations were performed to explore the ATX dosing in subjects with various CYP2D6 AS. A simultaneous pharmacokinetic modeling approach was used in which a model for ATX, 4-OH, and NDA in plasma and urine, and 2-COOH in urine was developed. Plasma ATX, 4-OH, and NDA were modeled using two-compartment models with first-order elimination. CYP2D6 AS was a significant determinant of ATX apparent oral clearance (CL/F), fraction metabolized to 4-OH, and systemic exposure of NDA. CL/F of ATX varied almost 7-fold across the CYP2D6 AS groups: AS 2: 20.02 L/hour; AS 1: 19.00 L/hour; AS 0.5: 7.47 L/hour; and AS 0: 3.10 L/hour. The developed model closely captures observed ATX, 4-OH, and NDA plasma and urine, and 2-COOH urine profiles. Application of the model shows the potential for AS-based dosing recommendations for improved individualized dosing.

Study Highlights

WHAT IS THE CURRENT KNOWLEDGE ON THE TOPIC?

☑ CYP2D6 phenotype significantly impact the disposition of atomoxetine (ATX) and its metabolites but the current label recommends to dose ATX regardless of CYP2D6 phenotype.

WHAT QUESTION DID THIS STUDY ADDRESS?

☑ The use of a pharmacometric modeling approach based on the available pharmacokinetic (PK) data of ATX and its metabolites might be helpful in quantifying the impact of CYP2D6 phenotype on the key PK parameters.

WHAT DOES THIS STUDY ADD TO OUR KNOWLEDGE?

☑ A model was developed to simultaneously characterize the PK profiles of ATX and its metabolites in both plasma and urine. The simulation performed suggested that subjects with CYP2D6 activity score (AS) ≥ 0.5 exhibit much lower exposures as measured by maximum concentration and area under the curve from zero to 24 hours at the ninth dosing day, under the clinical recommended 0.5 mg/kg once daily dose of ATX.

HOW MIGHT THIS CHANGE CLINICAL PHARMACOLOGY OR TRANSLATIONAL SCIENCE?

☑ Simulations suggested an increase in dose might be needed in subjects with CYP2D6 AS ≥ 1. The developed model is potentially useful to inform clinical decision of ATX dosing.

Atomoxetine (ATX) is used to treat attention-deficit/hyperactivity disorder (ADHD) and has been approved for use in children, adolescents, and adults.[1] ATX is well-absorbed after oral administration and is primarily cleared from the body by oxidative metabolism via the highly polymorphic drug metabolizing enzyme cytochrome P450 2D6 (CYP2D6). CYP2D6 is the primary

[1]Department of Experimental and Clinical Pharmacology, College of Pharmacy, University of Minnesota, Minneapolis, Minnesota, USA; [2]Division of Clinical Pharmacology, Toxicology, and Therapeutic Innovation, Department of Pediatrics, Children's Mercy Kansas City and University of Missouri-Kansas City, Kansas City, Missouri, USA; [3]Department of Pharmacy Practice and Pharmaceutical Sciences, University of Minnesota College of Pharmacy, Duluth, Minnesota, USA; [4]Present address: Gilead Sciences, Inc., Forest City, California, USA; [5]Present address: Metrum Research Group, Tariffville, Connecticut, USA. *Correspondence: Jacob T. Brown (jtbrown@d.umn.edu)

Received August 7, 2023; accepted December 12, 2023. doi:10.1002/cpt.3155

enzyme responsible for the formation of therapeutically active 4-hydroxyatomoxetine (4-OH) which is subsequently eliminated into the urine as conjugated metabolites.[2] To a smaller extent, ATX is also metabolized by CYP2C19 to form the inactive metabolite *N*-desmethylatomoxetine (NDA), which is further metabolized via CYP2D6 to form 4-OH *N*-desmethylatomoxetine (4-OH-NDA).[2]

The enzymatic activity of CYP2D6 is determined by genetic polymorphisms resulting in a range of function, including poor metabolizer (PM), intermediate metabolizer, normal metabolizer (NM), and ultrarapid metabolizer (UM).[3] Whereas CYP2D6 NMs can possess a range of variants contributing to fully functional CYP2D6 activity, CYP2D6 PMs lack catalytically active protein and metabolize atomoxetine much more slowly. Pharmacokinetic (PK) studies in adults reported an average 10-fold lower apparent oral clearance (CL/F) and a prolonged terminal half-life of ATX in PMs compared with non-PMs.[3,4] Consequently, systemic exposure as assessed by area under the curve (AUC) is, on average, 8–10-fold greater in PMs compared with non-PMs in both children and adults,[3,4] although variability at the individual patient level has been observed to be at least 30-fold.[5,6]

CYP2D6 genetic variation can range from non-functional or partial activity alleles to multiple copies of fully functional alleles. As a result, genetic polymorphisms of CYP2D6 produce the aforementioned four primary phenotypes that can have significant clinical implications.[7,8] Although the ATX product label recommends a common weight-based starting dose of 0.5 mg/kg/day in all children < 70 kg, regardless of *CYP2D6* genotype,[9] dosing ATX without accounting for CYP2D6 phenotypes may result in more frequent adverse events in PMs as compared with non-PMs[10] and an increased risk in inadequate therapeutic response for normal or UMs.[8,11] Thus, it is critical that factors with large effects on the dose-exposure relationship are identified and translated into dosing recommendations to ensure optimal therapeutic benefit in all patients, pediatric and adult.

We applied the concept of "activity score" (AS)[5,6] to conduct a genotype-stratified PK study of ATX in children and adolescents with ADHD to determine the magnitude of the CYP2D6 genotype effect on the dose-exposure relationship of ATX and its metabolites.[5] The CYP2D6 AS generally ranges from 0 to 3, with a higher score representing a higher CYP2D6 metabolic capacity.[12] The primary objective of this study was to develop a comprehensive model to characterize the disposition of ATX and its metabolites (4-OH, NDA, and 2-COOH) in children and adolescents with ADHD. The developed model has been applied to explore recommendations for dosage adjustments based on CYP2D6 genotype-predicted phenotype according to the current weight-based dosing guidelines.[9]

METHODS

Study population

This was a single-center, open-label study approved by the Institutional Review Board at Children's Mercy Kansas City. The details of the study population are published in our previous manuscript.[5] Briefly, patients were eligible for the study if they had a confirmed diagnosis of ADHD and previously participated in a longitudinal phenotyping study wherein *CYP2D6* genotype was determined. Children and adolescents ($n = 23$) between 9 and 17 years of age were studied. Participants were allowed to continue their daily medications during the study, but were excluded if they were currently taking ATX, known CYP2D6 inhibitors, had any known serious structural cardiac abnormalities, any flu like symptoms within 14 days, diagnosis of inflammatory bowel disease or Crohn's disease, or those with any hepatic and/or renal insufficiency. All study participants signed written consent with parental written permissions.

Study design

A more detailed description of the study design is provided in our previous single-dose study.[5] Briefly, following full-body examination, participants were admitted to the pediatric research unit and dosed to mimic the clinical setting such that each participant < 70 kg received a single capsule of the available dosage forms to provide a dose at or near the recommended starting dose of 0.5 mg/kg; participants > 70 kg were given a maximum of 40 mg ATX single dose. A baseline pre-dose blood sample was obtained and the patients then received their ATX dose. Following the dose, serial blood samples were obtained at 0.5, 1, 2, 4, 6, 8, 12, 16, 20, and 24 hours. For participants with a CYP2D6 AS of 0 (i.e., PMs), 48- and 72-hour plasma samples were also collected due to the extended half-life of ATX and its metabolites. Urine was collected for a 24-hour interval in participants with a CYP2D6 AS > 0 and for a 72-hour interval in participants with a CYP2D6 AS of 0.

Genotyping and bioanalytical methods

The detailed procedure of *CYP2D6* genotyping is described in detail in previous manuscripts.[5,6,13–16] The assayed *CYP2D6* alleles (defined according to Human Cytochrome P450 (CYP2D6) Allele Nomenclature Database at https://www.pharmvar.org/htdocs/archive/cyp2d6.htm) were converted to CYP2D6 activity scores according to Gaedigk *et al*.[6]

ATX, 4-OH (unconjugated and total), and NDA concentrations were measured in plasma and ATX, 4-OH, NDA, and 2-COOH concentrations were measured in urine samples and analyzed by a validated assay using a ultra-high-performance liquid chromatography-tandem mass spectrometry method developed in-house as described in the previous study.[5,17] The 4-OH plasma concentrations were measured before and after glucuronidase treatments and were referred to as unconjugated and total 4-OH, respectively.

PK modeling

Nonlinear mixed-effect modeling (NONMEM 7.5; ICON Development Solutions, Ellicott City, MD) was performed to analyze ATX, 4-OH, and NDA plasma and urine, and 2-COOH urine concentrations obtained over 72 hours from children with ADHD ($n = 23$) following a single oral dose of ATX. First-order conditional estimation with interaction method was used. In the final models described below, between-subject variabilities (BSVs) were described by lognormal distributions. For the residual unexplained variability (RUV), proportional error models were used for each analyte. In each plasma sample collected, the concentrations of the parent compound and metabolites were measured. Thus, a level two (L2) data record was used in the dataset to group the observations measured from the same sample and account for the potential correlations.[18] Exploratory analyses and diagnostic graphics were performed in R (version 3.6.3) using RStudio (RStudio, PBC) following the procedure of Metrum Research Group example project[19] and Perl-speaks-NONMEM (PsN 4.9.0, Uppsala University, Uppsala, Sweden) under the Pirana interface.

A simultaneous PK modeling approach was used in which a model for plasma and urine ATX, 4-OH (unconjugated and total), NDA, and 2-COOH was developed (**Figure 1**). A detailed description of the model development process is provided in the Supplementary Materials (**Supplementary material: Model Development.docx**), along with the model codes in both NONMEM (**Supplementary material: NONMEM.lst file.pdf**) and mrgsolve (**Supplementary material: ATX-mrgsolve-model-guide.pdf**).

Model evaluations

The stability of the model fitting was evaluated by several factors, such as the successful model convergence, the successful execution of model covariance step, the plausibility of model parameter estimates, and the precision of model parameter estimates. Shrinkage was calculated for both eta (η) and epsilon (ε), as shown by Savic *et al.*[20] The final model fitting was assessed by standard diagnostic plots.[21] The precision of the final model parameters was evaluated using both the asymptotic standard errors estimated by model covariance step and the sampling-importance-resampling (SIR)-based 95% confidence intervals (CIs).[22,23] The predictions of the final model were evaluated following the procedure of prediction-corrected visual predictive checks (pcVPC) with 1,000 simulation replicates.[24]

Model-based analysis

Following the model development, the fractions of metabolism through 4-OH (fm 4-OH), NDA (fm NDA), and 2-COOH (fm 2-COOH) and the fraction of renal excretion as unchanged ATX (fe) were calculated using the estimated typical model parameters. The overall clearance (CL) of ATX (i.e., the sum of CL/F across all elimination pathways, including renal excretion as unchanged ATX, and 4-OH, NDA, and 2-COOH mediated metabolism) was also computed with the estimated typical model parameters for participants with each CYP2D6 AS.

Assuming a 0.5 mg/kg q.d. ATX dosing, the effects of CYP2D6 AS and body weight on ATX CL/F and steady-state area under the curve over a dosing interval (AUC_{ss}) were assessed using a forest plot approach, where the covariate effect of interest was varied individually at each time while keeping the other covariates as constant (*ceteris paribus*), with the parameter uncertainty derived from SIR analysis. The population with a CYP2D6 AS of 2 (i.e., normal metabolizers[25]) and body weight of 70 kg was used as the reference population. The AUC_{ss} was calculated using Eq. 1 as shown below considering linear PK of ATX.

$$\mathrm{AUCss} = \frac{F1 * \mathrm{DOSE}}{\mathrm{CL}} \quad (1)$$

Simulations

Simulations were performed using open-source R package mrgsolve (version 0.11.1).[26] The final ATX model was translated from NONMEM to mrgsolve. The mrgsolve model validation procedure was performed to ensure the correct model translation.[27]

Population simulations were performed with BSV, but without RUV, to ensure an accurate calculation of drug exposure metrics (such as maximum concentration (C_{max})). One hundred ($N = 100$) virtual subjects were simulated for each CYP2D6 AS group (0, 0.5, 1, 2, and 3). The body weight of the virtual subjects was sampled from a truncated normal distribution with a mean of 67.8 kg and a standard deviation (SD) of 27.6 kg, both of which were derived from the analysis dataset. Three ATX dosing regimens were evaluated: (i) 0.5 mg/kg once daily (q.d.); (ii) 1.2 mg/kg q.d.; and (iii) 1.4 mg/kg q.d. The PK exposures of pharmacologically active analytes (ATX and unconjugated 4-OH), including both

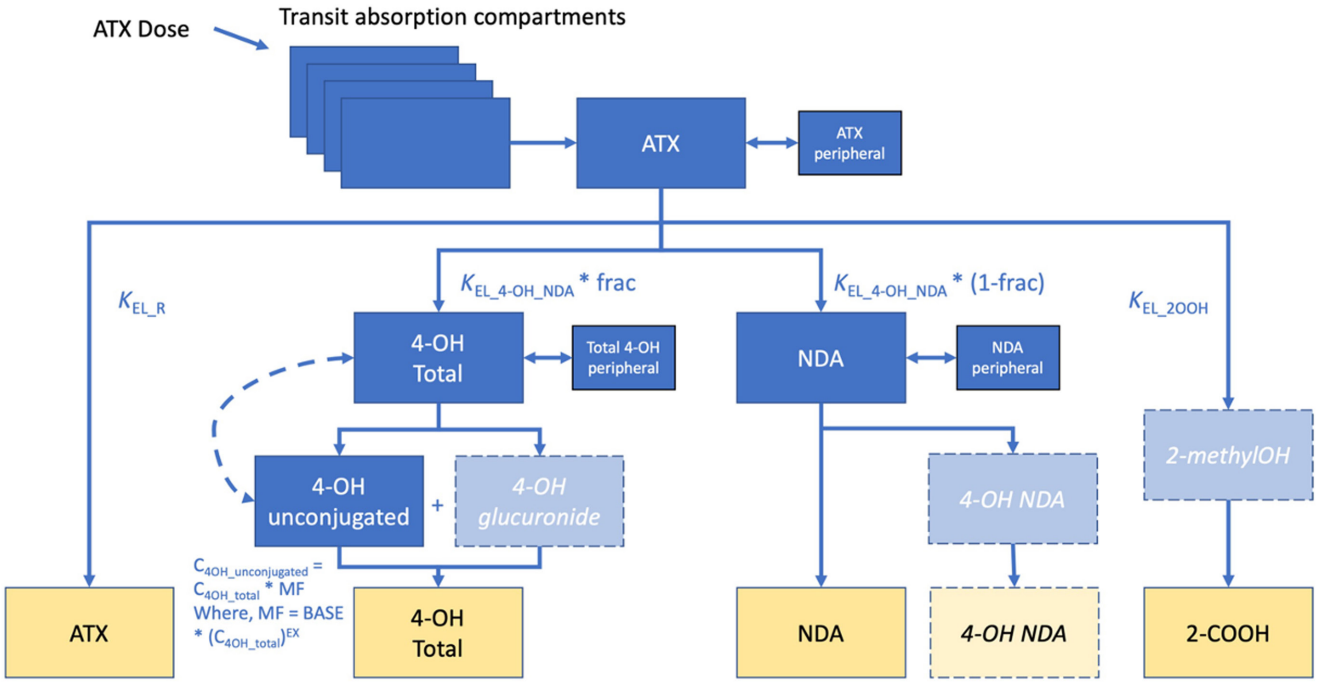

Figure 1 Final model structure. Dash line means no mass transfer. Solid boxes and colors represent analytes measured in plasma (blue) and urine (gold). Light shaded with dashed lines represent analytes not measured. 4-OH glucuronide can theoretically be calculated as total minus unconjugated (aglycone). 2-COOH, 2-carboxymethylatomoxetine; 4-OH, 4-hydroxyatomoxetine; ATX, atomoxetine; BASE, base in the power function; C_{4OH_total}, total 4-OH concentration in plasma; $C_{4OH\_unconjugated}$, unconjugated 4-OH concentration in plasma; EX, exponent in the power function; frac, fraction of $K_{EL\_4OH\_NDA}$ undergo 4-OH pathway; $K_{EL\_4OH\_NDA}$, metabolic elimination rate constant of ATX as either 4-OH or NDA; K_{EL_COOH}, renal elimination rate constant of ATX as 2-COOH; K_{EL_R}, renal elimination rate constant of ATX as unchanged drug; MF, multiplication factor; NDA, *N*-desmethylatomoxetine.

the maximal concentration at each dosing day (C_{max}) and the area under the curve over 24-hour interval (AUC_{0-24}) were summarized at days 1, 5, and 9 (day 9 was considered as the steady-state). The day 9 ATX and 4-OH C_{max} and AUC_{0-24} were used as the PK exposure metrics for comparison under different ATX dosing regimens across various CYP2D6 AS groups. A 400 ng/mL steady-state ATX C_{max} was used as the therapeutic target related to drug efficacy for comparison as suggested by the ATX/CYP2D6 Clinical Pharmacogenetics Implementation Consortium (CPIC) guideline.[12,28]

RESULTS

Data

Demographic characteristics of the study participants are provided in **Table S1**. The analysis dataset included 23 subjects with a mean age of 14.2 years (SD: 2.54 years), a mean body weight of 67.8 kg (SD: 27.6 kg) and a mean body mass index of 23.9 kg/m^2 (SD: 6.42 kg/m^2). Among the 23 study participants, the CYP2D6 ASs were grouped as 0 ($n = 4$), 0.5 ($n = 3$), 1 ($n = 8$), 2 ($n = 7$), and 3 ($n = 1$). One participant with a CYP2D6 AS of 3 was combined with participants with CYP2D6 AS of 2 as a single category during modeling, because only one participant had a CYP2D6 AS of 3 in the analysis dataset. Overall, 237 ATX plasma samples, 234 NDA plasma samples, 220 4-OH plasma samples, and 230 2-COOH plasma samples were included in the analyses.

Spaghetti plots of individual dose normalized plasma concentrations of ATX, total and unconjugated 4-OH, and NDA are shown in **Figure 2**. The exposure of ATX is shown to increase as the AS of CYP2D6 decreases. The CYP2D6 phenotype-dependent exposures are also observed in the 4-OH (unconjugated and total) and NDA PK profiles. Urine measurements vs. CYP2D6 AS are shown in **Figure S1**. Comparing across the ATX and 4-OH urine amounts collected over a 24-hour interval, CYP2D6 phenotype-dependent exposures were also observed.

PK model parameters

The final PK model parameter estimates, their relative standard error, BSV, RUV, shrinkage, and SIR-based 95% CIs for ATX, NDA, 4-OH, and 2-COOH are provided in **Table 1**. After including allometrically scaled CL/F and volume of distribution (V/F) of all analytes using body weight, CYP2D6 AS was a significant determinant of ATX relative bioavailability, fraction of ATX (other than renal ATX and 2-COOH elimination) metabolized (%) to 4-OH, and ATX CL/F. Study participants with a CYP2D6 AS of ≥ 1 had an ~9-fold higher 4-OH and NDA mediated ATX CL/F compared with CYP2D6 AS 0 subjects. Similarly, after allometrically scaling of NDA and 4-OH CL/F and V/F by body weight, a significant improvement to the model was realized with the inclusion of CYP2D6 AS on the NDA CL/F (**Table 1**). Albumin and hematocrit were not found to have any statistically significant ($P > 0.001$) effect on any of the final model parameter estimates. Generally, the parameter estimates suggest that CYP2D6 AS is a significant covariate on several metabolic processes of ATX disposition, such as bioavailability, parent compound elimination, and metabolite (4-OH) formation, and metabolite (NDA) elimination (**Table 1**).

Model evaluations

The final model was able to converge with the successful implementation of the model covariance step (**Supplementary**

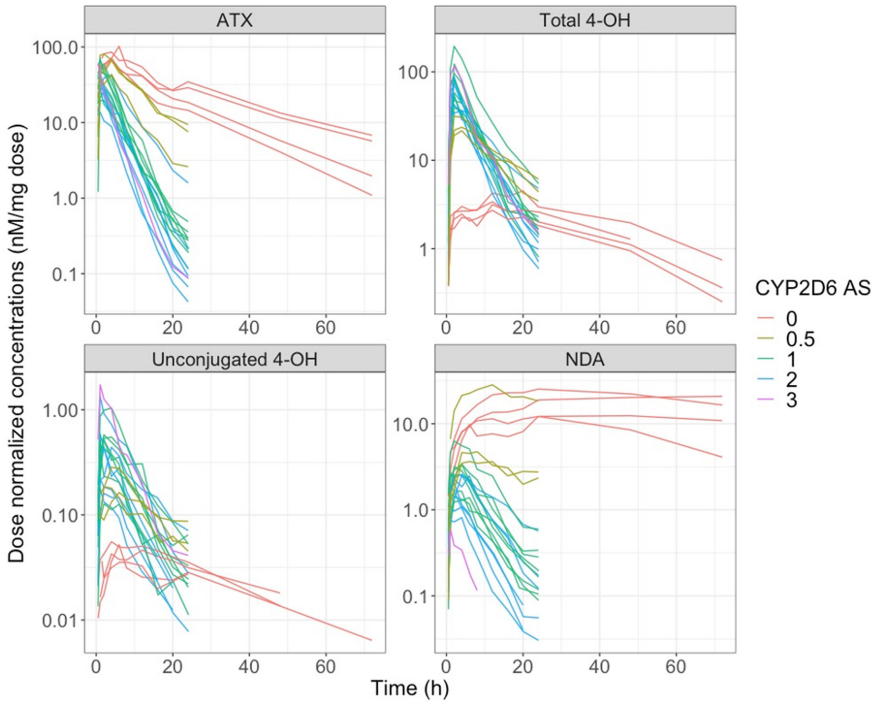

Figure 2 Dose normalized plasma concentration of ATX, total 4-hydroxyatomoxetine (total 4-OH), unconjugated 4-hydroxyatomoxetine (unconjugated 4-OH), *N*-desmethylatomoxetine (NDA) and 2-carboxymethylatomoxetine (2-COOH) vs. time. Color represents CYP2D6 AS. AS, activity score; ATX, atomoxetine.

Table 1 Final PK parameter estimates, precisions, and shrinkages

Parameter (unit)	Estimate (RSE%)	SIR median (95% CI)	Shrinkage %[a]	Notes
Oral ATX PK Parameters (2-compartment)				
F1 (fraction, unitless) (stratified by *CYP2D6* phenotype)				Relative bioavailability
CYP2D6 AS ≤0.5	1 FIXED	—	—	—
CYP2D6 AS 1	0.895 (4)	0.894 (0.835, 0.961)	—	—
CYP2D6 AS ≥2	0.812 (4)	0.811 (0.756, 0.868)	—	—
CL/F (L/hour) (stratified by *CYP2D6* phenotype)				Clearance of ATX mediated by 4-OH and NDA pathways
CYP2D6 AS 0	$2.12\times(WT/70)^{0.75}$ (17)	2.10 (1.64, 2.66)	—	—
CYP2D6 AS 0.5	$6.49\times(WT/70)^{0.75}$ (20)	6.49 (3.56, 11.0)	—	—
CYP2D6 AS 1	$18.0\times(WT/70)^{0.75}$ (17)	17.9 (10.3, 29.5)	—	—
CYP2D6 AS ≥2	$19.0\times(WT/70)^{0.75}$ (20)	19.1 (10.7, 32.2)	—	—
V/F (L)	$75.7\times(WT/70)^{1.0}$ (7)	75.5 (67.5, 84.5)	—	Volume of distribution of ATX
Q/F (L/hour)	$0.487\times(WT/70)^{0.75}$ (13)	0.48 (0.38, 0.60)	—	Intercompartment clearance of ATX
V2/F (L)	$8.57\times(WT/70)^{1.0}$ (38)	8.43 (5.64, 15.4)	—	Peripheral volume of distribution of ATX
KATR (1/hour)	7.35 (8)	7.28 (6.34, 8.57)	—	Transit rate constant of ATX
KELR (1/hour)	0.000754 (14)	0.000763 (0.000587, 0.000913)	—	Renal elimination rate constant of ATX
F_m4-OH (fraction, unitless) (stratified by *CYP2D6* phenotype)				Fraction of ATX (Other than renal and 2-COOH eliminations) metabolized (%) to 4-OH
CYP2D6 AS 0	0.359 (8)	0.360 (0.316, 0.414)	—	—
CYP2D6 AS 0.5	0.740 (5)	0.740 (0.677, 0.797)	—	—
CYP2D6 AS 1	0.923 (1)	0.924 (0.905, 0.941)	—	—
CYP2D6 AS ≥2	0.932 (1)	0.932 (0.916, 0.947)	—	—
4-OH PK Parameters (2-compartment)				
V/F (L)	$7.81\times(WT/70)^{1.0}$ (11)	7.76 (6.27, 9.34)	—	Volume of distribution of 4-OH
Q/F (L/hour)	$1.60\times(WT/70)^{0.75}$ (18)	1.60 (1.17, 2.22)	—	Intercompartment clearance of 4-OH
V2/F (L)	$11.4\times(WT/70)^{1.0}$ (11)	11.5 (9.60, 13.7)	—	Peripheral volume of distribution of 4-OH
CL/F (L/hour)	$7.82\times(WT/70)^{0.75}$ (5)	7.82 (7.15, 8.52)	—	Clearance of 4-OH
Unconjugated 4-OH PK Parameters (power function: $C_{4\text{-OH}}$ (unconjugated) = BASE × $C_{4\text{-OH}}$ (total)^{EX})				
EX (unitless)	−0.182 (12)	−0.184 (−0.221, −0.140)	—	Exponent
BASE (unitless)	0.0284 (14)	0.0285 (0.0218, 0.0357)	—	Base
NDA PK Parameters (2-compartment)				
CL/F (L/hour) (stratified by *CYP2D6* phenotype)				Metabolic clearance of NDA
CYP2D6 AS 0	$0.851\times(WT/70)^{0.75}$ (35)	0.837 (0.488, 1.55)	—	—
CYP2D6 AS 0.5	$3.54\times(WT/70)^{0.75}$ (59)	3.46 (0.703, 15.5)	—	—
CYP2D6 AS 1	$10.6\times(WT/70)^{0.75}$ (46)	10.5 (2.83, 39.4)	—	—
CYP2D6 AS ≥2	$18.0\times(WT/70)^{0.75}$ (43)	17.5 (4.63, 64.3)	—	—
V/F (L)	$12.0\times(WT/70)^{1.0}$ (17)	11.9 (9.23, 15.4)	—	Volume of distribution of NDA
Q/F (L/hour)	$7.09\times(WT/70)^{0.75}$ (18)	6.99 (5.25, 9.33)	—	Intercompartment clearance of NDA
V2/F (L)	$34.9\times(WT/70)^{1.0}$ (14)	34.7 (27.2, 41.7)	—	Peripheral volume of distribution of NDA
KELR (1/hour)	0.00211 (19)	0.00214 (0.00152, 0.00281)	—	Renal elimination rate constant of NDA

(Continued)

Table 1 (Continued)

Parameter (unit)	Estimate (RSE%)	SIR median (95% CI)	Shrinkage %[a]	Notes
2-COOH PK Parameters (urine only)				
KEL_COOH (1/hour)	0.0122 (10)	0.0123 (0.0103, 0.0145)	—	Elimination rate constant of ATX through 2-COOH pathway
BSV, CV%				CV % was calculated as $\sqrt{e^{\omega^2}-1}$
BSV ATX				
CL/F	34.9 (18)	34.7 (26.1, 46.5)	1	—
COV (CL/F, V/F)	0.0529[b]	0.0497 (0.0242, 0.0971)	—	Correlation between CL/F and V/F
V/F	27.3 (18)	27.0 (20.0, 37.8)	5	—
KATR	37.0 (17)	37.0 (26.5, 51.9)	5	—
BSV 4-OH				
CL/F	17.1 (18)	17.1 (12.5, 23.6)	7	—
V/F	40.4 (22)	40.9 (25.5, 60.5)	13	—
BSV unconjugated 4-OH				
EX	14.5 (86)	14.3 (1.77, 34.3)	51	—
BASE	36.6 (22)	36.8 (23.3, 50.9)	8	—
BSV NDA				
CL/F	86.7 (16)	87.7 (63.1, 129)	0.4	—
V/F	32.4 (31)	33.2 (15.3, 52.3)	17	—
RUV, CV%				CCV% was calculated as $\sqrt{\sigma^2}$
Prop RUV, CCV%				Proportional errors
ATX plasma	21.3 (6)	21.5 (19.3, 23.7)	8	—
4-OH plasma	29.3 (6)	29.3 (26.5, 32.8)	9	—
Unconjugated 4-OH plasma	20.1 (6)	20.1 (17.9, 22.5)	9	—
NDA plasma	21.8 (6)	21.8 (19.6, 24.5)	11	—
ATX urine	60.1 (23)	59.3 (43.4, 83.6)	1	—
4-OH urine	14.3 (17)	14.5 (12.0, 19.0)	1	—
NDA urine	51.4 (22)	51.1 (37.1, 75.1)	3	—
COOH urine	48.4 (21)	47.7 (36.1, 67.8)	1	—

2-COOH, 2-carboxymethylatomoxetine; 4-OH, 4-hydroxyatomoxetine; AS, activity score; ATX, atomoxetine; BSV, between-subject variability; CCV, constant coefficient of variation; CI, confidence interval; CL/F, calculated oral clearance; CV, coefficient of variation; NDA, *N*-desmethylatomoxetine; PK, pharmacokinetic; RSE, relative standard errors; RUV, residual unexplained variability; SIR, sampling importance resampling; V/F, volume of distribution; WT, weight in kg.
[a]Shrinkage was calculated for both η and ε as shown by Savic *et al.*[20]
[b]Value was presented as correlation.

material: NONMEM.lst file.pdf). The final model parameters were estimated with reasonable precision (i.e., < 100%, with majority of estimates < 50%) according to both the asymptotic standard errors calculated from the model covariance step and the SIR-based 95% CIs (**Table 1**). The overall goodness-of-fit plots indicated little reason to reject the model (**Figures S2 and S3**). The VPCs in plasma and urine are shown in **Figures S5–S9**, respectively. The prediction-corrected 5th, 50th, and 95th observational percentiles for most time bins were within the prediction intervals of the prediction-corrected 5th, 50th, and 95th simulated percentiles of ATX, unconjugated and total 4-OH, NDA, and 2-COOH in plasma and/or urine, which indicates the model predicted the observed data reasonably well.

Model-based analysis

In subjects with a CYP2D6 AS > 0, metabolic formation of 4-OH is the predominant elimination pathway of ATX. However, in subjects with a CYP2D6 AS of 0, NDA mediated metabolic elimination (when assuming ATX is completely eliminated through ATX unchanged, 4-OH, NDA, and 2-COOH) becomes the predominant pathway. As CYP2D6 AS decreases, the fraction of 4-OH mediated metabolic elimination decreases and the fraction of NDA and 2-COOH mediated metabolic elimination increases (**Figure 3a**). As expected, the calculated overall ATX CL/F (i.e., the sum of CL/F across all elimination pathways, including renal excretion as unchanged ATX, and 4-OH, NDA, and 2-COOH mediated metabolism) decreases as the CYP2D6 AS decreases (**Figure 3b,c**).

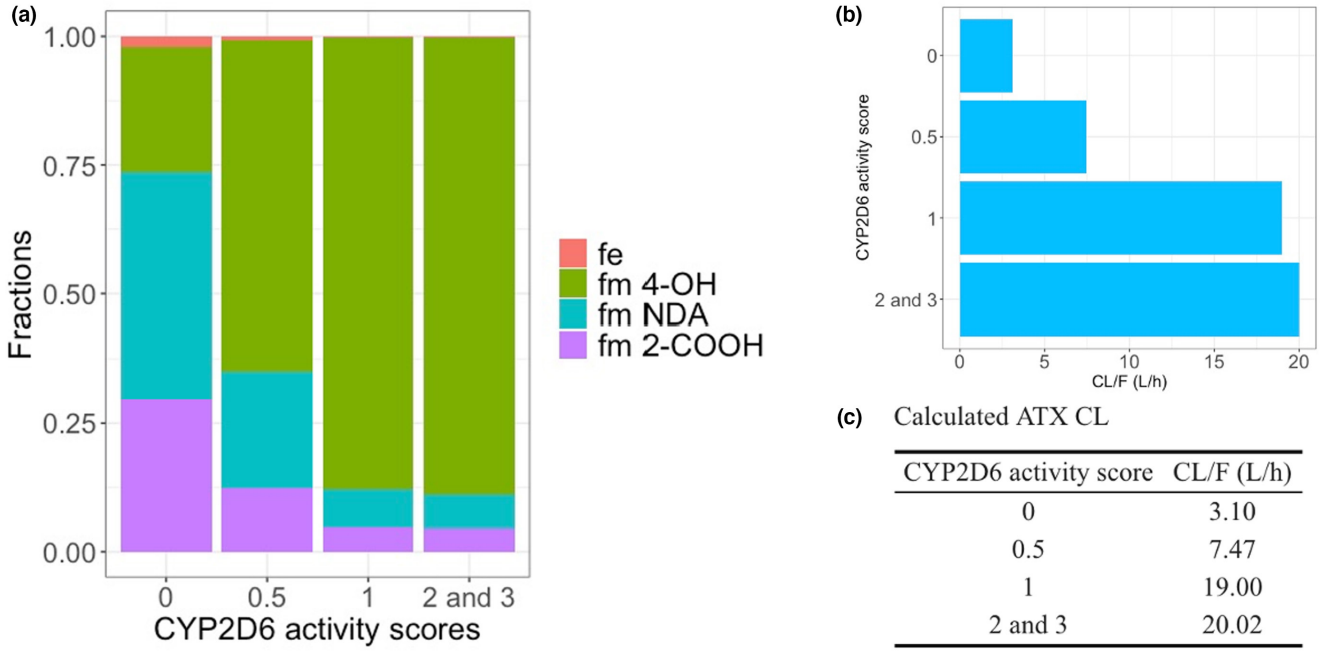

(c) Calculated ATX CL

CYP2D6 activity score	CL/F (L/h)
0	3.10
0.5	7.47
1	19.00
2 and 3	20.02

Figure 3 Model-based analysis of the ATX elimination profiles. (**a**) Fraction of each elimination pathway vs. CYP2D6 activity scores. Color represents different elimination pathway. Graphical (**b**) and tabulated (**c**) summary of the CL/F of ATX vs. CYP2D6 activity scores based on the typical parameter estimates of the final model. 2-COOH, 2-carboxymethylatomoxetine; 4-OH, 4-hydroxyatomoxetine; ATX, atomoxetine; CL/F, calculated oral clearance; NDA, *N*-desmethylatomoxetine.

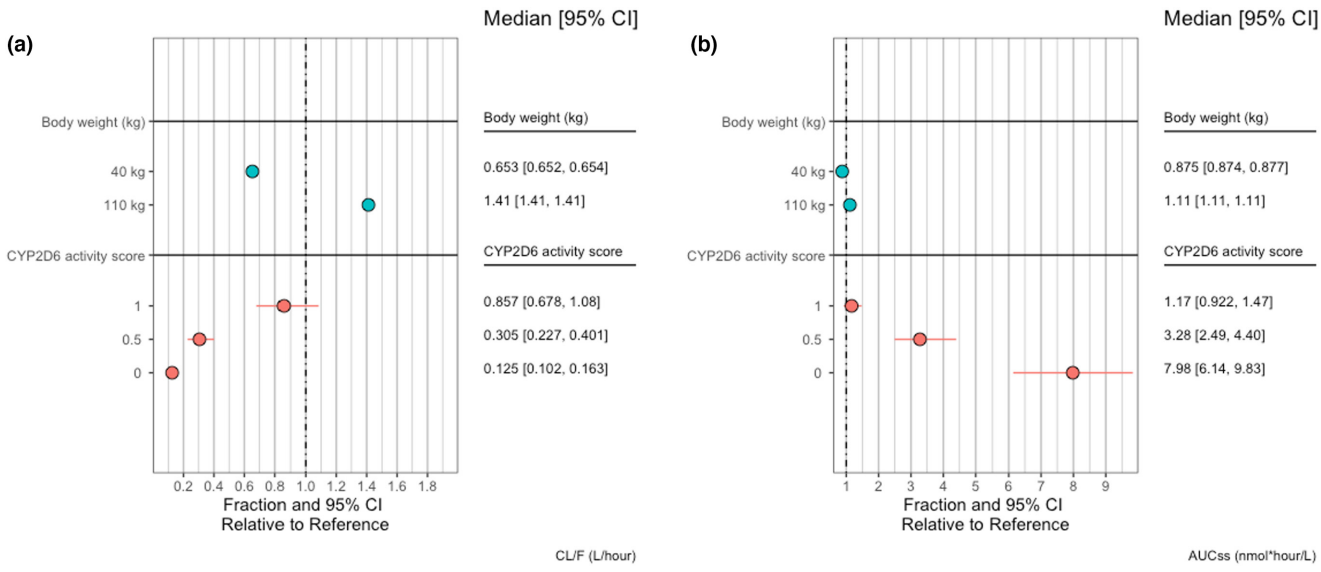

Figure 4 The effects of CYP2D6 activity scores and body weight on (**a**) ATX oral clearance (CL/F) and (**b**) AUC_{ss}. The dosing regimen of atomoxetine is 0.5 mg/kg once daily (Q.D). The reference population is subjects with CYP2D6 activity score of 2 and body weight of 70 kg. ATX, atomoxetine; AUC_{ss}, steady-state area under the curve over a dosing interval; CI, confidence interval; CL/F, calculated oral clearance; C_{max}, maximum concentration.

The covariate effects of body weight and CYP2D6 AS were assessed using a forest plot approach (Figure 4). The ATX CL/F in subjects with 40 kg body weight and 110 kg body weight are 0.653- (95% CI: 0.652, 0.654) and 1.41-fold (95% CI: 1.41, 1.41) of the ATX CL/F in subjects with 70 kg of body weight, respectively. The ATX CL/F in subjects with CYP2D6 AS of 0, 0.5, and 1 are 0.125 (95% CI: 0.102, 0.163), 0.305 (95% CI: 0.227, 0.401), and 0.857 (95% CI: 0.678, 1.08) of that in subjects with CYP2D6 AS of 2, respectively (Figure 4a). Assuming a weight-based dosing regimen of 0.5 mg/kg q.d., the effects of low (40 kg) and high (110 kg) body weight on AUC_{ss} are smaller as compared with their effects on ATX CL/F, which are 0.875- (95% CI: 0.874, 0.877)

and 1.11-fold (95% CI: 1.11, 1.11) of the ATX AUC_{ss} in subjects with 70 kg of body weight, respectively. In contrast, subjects with CYP2D6 AS of 0, 0.5, and 1 have ATX AUC_{ss} 7.98- (95% CI: 6.14, 9.83), 3.28- (95% CI: 2.49, 4.40), and 1.17-fold (95% CI: 0.922, 1.47) of that in subjects with CYP2D6 AS of 2 (**Figure 4b**). Collectively, these results showed both body weight and CYP2D6 AS could profoundly impact the CL/F of ATX. Whereas the application of weight-based ATX dosing according to current ATX dosing guideline could reduce the impact of body weight, it cannot reduce the impact of CYP2D6 AS.

Simulations

The translated ATX mrgsolve model reproduced the population prediction of the original NONMEM model, validating the use of ATX mrgsolve model for simulations (**Figure S4**). The simulated C_{max} and AUC_{0-24} of the pharmacologically active analytes, ATX, and unconjugated 4-OH, were summarized on days 1, 5, and 9 in subjects with each CYP2D6 AS under each dosing regimen (**Tables S2–S4**). Overall, the ATX exposures are higher in subjects with lower CYP2D6 AS (**Tables S2–S4**; **Figure S10**). The unconjugated 4-OH exposures are lower in subjects with a CYP2D6 AS < 1 and are similar once CYP2D6 ASs are ≥ 1 (**Tables S2–S4**; **Figure S11**). The C_{max} and AUC_{0-24} at day 9 (i.e., steady-state) was further investigated for exposure comparison under various ATX dosing regimens in subjects with different CYP2D6 phenotypes. Under the recommended starting dose of 0.5 mg/kg q.d. of ATX, subjects with CYP2D6 AS of 1, 2, and 3 have much lower steady-state ATX exposures (i.e., C_{max} and AUC_{0-24} at day 9) as compared with the subjects with CYP2D6 AS of 0 (**Figures 5a,c**; **Table 2**). Using 400 ng/mL steady-state C_{max} as the therapeutic target of ATX,[12,28] the majority of the subjects with a CYP2D6 AS of 1, 2, and 3 failed to meet this concentration threshold under the 0.5 mg/kg q.d. of ATX as compared with the subjects with CYP2D6 AS of 0 and 0.5 (**Figure 5a**). In contrast, under the recommended starting dose of 0.5 mg/kg q.d. of ATX, subjects with CYP2D6 AS of 1, 2, and 3 have much higher unconjugated 4-OH steady-state exposures (i.e., C_{max} and AUC_{0-24} at day 9) as compared with the subjects with a CYP2D6 AS of 0 (**Figure 5b,d**). To match the day 9 (steady-state) ATX C_{max} achieved in subjects with a CYP2D6 AS of 0 under the 0.5 mg/kg q.d. dose of ATX, subjects with a CYP2D6 AS ≥ 1 require an ~ 1.2 mg/kg q.d. dose of ATX (**Figure 5a**, **Table 2**).

DISCUSSION

In the current analysis, a nonlinear mixed-effect modeling approach was applied to develop a comprehensive population PK model characterizing ATX and its metabolites simultaneously in

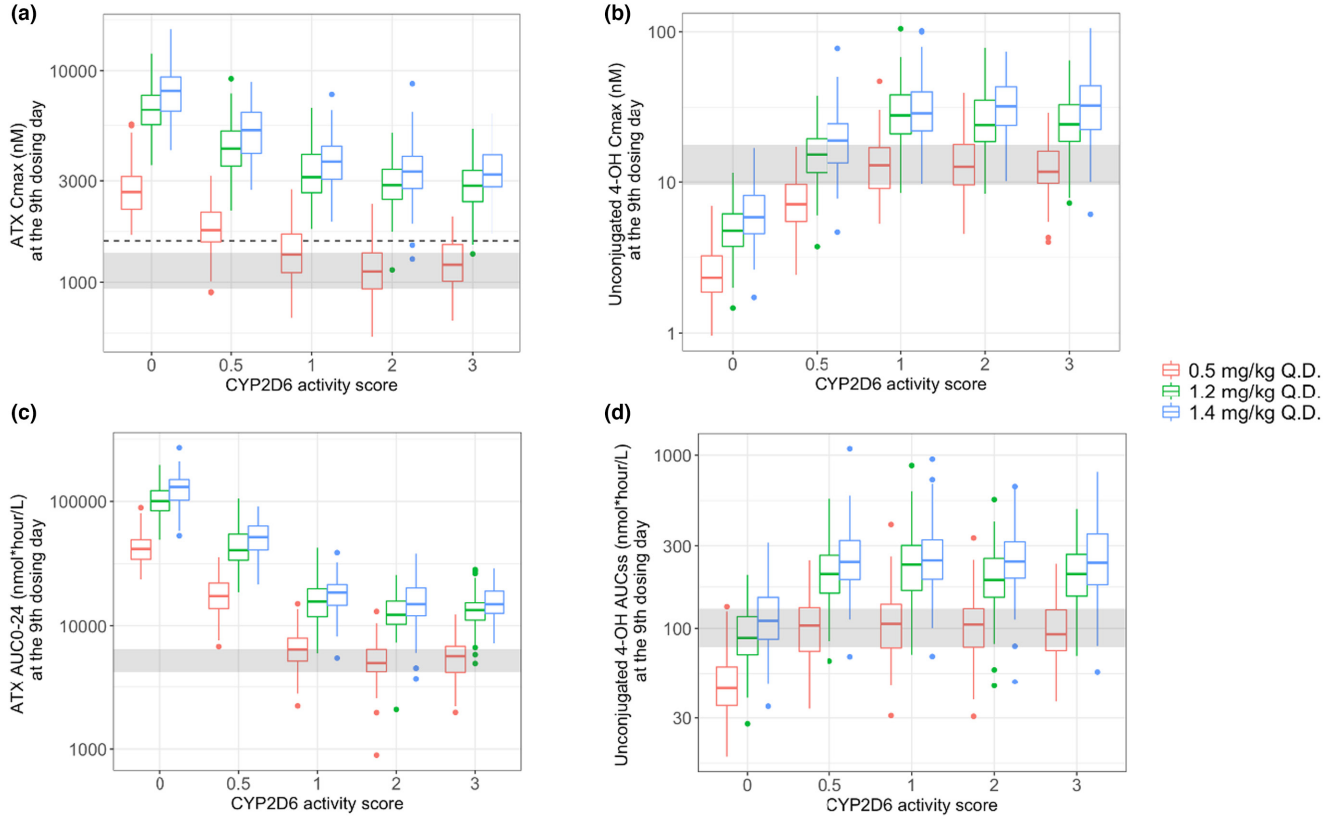

Figure 5 ATX exposures (C_{max} (**a**) and AUC_{0-24} (**c**) at the 9th dosing day) and 4-hydroxyatomoxetine (4-OH) exposures (C_{max} (**b**) and AUC_{0-24} (**d**) at the 9th dosing day) vs. CYP2D6 activity score under various ATX dosing regimens. Color represents dosing regimens of ATX. The dash line on panel a indicates the 400 ng/mL steady-state C_{max} therapeutic target suggested by atomoxetine CPIC guideline.[12] Shaded areas represent the exposures achieved by the CYP2D6 AS 2 reference group. q.d., once daily. ATX, atomoxetine; AS, activity score; AUC_{0-24}, area under the curve from 0 to 24 hours; C_{max}, maximum concentration; CPIC, Clinical Pharmacogenetics Implementation Consortium.

Table 2 Steady-state PK exposures of atomoxetine simulated for each CYP2D6 activity score group (*N* = 100) with respective dosing regimen

Dosing regimens	CYP2D6 AS: 0	CYP2D6 AS: 0.5	CYP2D6 AS: 1	CYP2D6 AS: 2	CYP2D6 AS: 3
C_{max} (nM)					
0.5 mg/kg q.d.	2,793.52 (764.173)	1,843.57 (459.962)	1,404.88 (403.868)	1,184.27 (317.374)	1,259.25 (318.625)
1.2 mg/kg q.d.	6,733.19 (1,774.97)	4,447.99 (1,301.20)	3,366.92 (1,053.05)	2,974.44 (738.850)	2,929.32 (751.563)
1.4 mg/kg q.d.	8,114.16 (2,119.10)	5,280.77 (1,422.05)	3,786.87 (974.183)	3,514.09 (1,141.99)	3,402.16 (880.341)
AUC_{0-24} (nmol*hour/L)					
0.5 mg/kg q.d.	43,664.9 (12,759.3)	18,536.1 (6,351.54)	6,683.98 (2,229.20)	5,402.46 (1,952.23)	5,844.74 (2,060.08)
1.2 mg/kg q.d.	105,380 (30,469.6)	44,776.8 (16,557.3)	16,691.7 (6,824.17)	13,168.5 (4,215.10)	13,827.1 (4,515.98)
1.4 mg/kg q.d.	128,236 (37,403.5)	52,073.5 (16,073.6)	18,567.9 (5,260.01)	16,227.9 (6,603.89)	15,769.6 (4,866.33)

Values are shown as mean (SD).
AS, activity score; AUC_{0-24}, area under the curve across the dosing day (24-hour interval); C_{max}, maximum concentration; PK, pharmacokinetic.

plasma and urine. We then used this model to explore the dose-exposure relationship of ATX following chronic administration in children and adolescents with ADHD. The covariate effect of CYP2D6 AS on the PK parameters of ATX and its metabolites was evaluated in the final model. Finally, the developed PK model demonstrated the capability of simulation to potentially inform ATX clinical dosing decisions in the future.

It is well known that the genetic polymorphism of CYP enzymes has the potential to impact the systemic exposure of many drugs.[29] For ATX, the final PK model estimated a lower ATX bioavailability in CYP2D6 AS ≥ 1 patients as compared with the CYP2D6 AS 0 and 0.5 patients following a single oral dose of 0.5 mg/kg (**Table 1**). The estimated ATX bioavailability in the CYP2D6 AS ≥ 1 groups were 89.5% and 81.2% of that in the CYP2D6 AS 0 and 0.5 patients, respectively. These differences in ATX bioavailability between CYP2D6 AS groups are consistent with the literature, and are primarily attributed to the different contributions of hepatic first-pass metabolism in subjects with different CYP2D6 phenotypes.[1,9] It should be noted that the model presented in this study can only estimate relative bioavailability, as it is based solely on PK profiles from oral administration of ATX. Therefore, assigning a relative bioavailability value of 1 to CYP2D6 AS 0 and 0.5 patients only implies that their bioavailability has been used as the reference group, not indicating their bioavailability is 100%.

The CYP2D6 AS 0 group showed significantly lower ATX and NDA CL/F values as compared with those with a CYP2D6 AS ≥ 0.5 (**Table 1**, **Figure 3b**). Although several CYP enzymes are capable of catalyzing the formation of 4-OH (e.g., CYP2D6, CYP3A4, and CYP2E1),[17] CYP2D6 is the primary enzyme responsible for the metabolic formation of therapeutically active 4-OH, the major metabolite of ATX.[1,12] Regardless of the CYP2D6 AS, 4-OH is subsequently eliminated into the urine as the conjugated metabolites. A smaller proportion of ATX is also metabolized by CYP2C19 to form the inactive metabolite NDA. The NDA can be further metabolized via CYP2D6 to form *N*-desmethyl 4-OH.[7,12] The dependence of metabolic formation of *N*-desmethyl 4-OH on CYP2D6 activity explained the CYP2D6 phenotype-dependent NDA CL/F values observed in this analysis (**Table 1**).

Additionally, our analysis found that the contribution of 4-OH to the overall metabolic elimination pathway decreased as the CYP2D6 AS (functional CYP2D6 activity) decreases (**Figure 3a**). Although the formation of 4-OH is the predominant ATX elimination pathway in CYP2D6 AS ≥ 0.5 patients, minor metabolic pathways dominate when CYP2D6 activity is compromised.[30,31] Frequently referred to as "shifting" or "shunting" in the literature, the issue is more related to loss of the quantitatively most important pathway. Consider a situation where CYP2D6, CYP2C19, and CYP2B6 are responsible for 75%, 15%, and 10% of the total clearance of a compound – in essence a "pie" of 100 units, with slices of 75, 15, and 10 units. When the CYP2D6 contribution is absent due to PM status or drug–drug inhibition, the "pie" is reduced in size to 25 units, with CYP2C19 and CYP2B6 representing 60% and 40%, respectively, of the total CL; these minor pathways now represent a larger fraction of the remaining CL, but the CL is still dramatically reduced. In this situation, however, the impact of genetic variation, drug–drug interactions and other factors affecting the activity of the minor pathways may be more pronounced than in the presence of the major CL pathway.

Covariate effects of body weight and CYP2D6 AS were evaluated using a forest plot approach (**Figure 4**). As expected, both body weight and the CYP2D6 AS significantly impact the ATX CL/F. Importantly, consistent with the previous studies,[3,4] our analysis showed CYP2D6 AS ≥ 1 patients exhibit 5–7-fold higher ATX CL/F than CYP2D6 AS 0 patients (**Figure 4a**). In contrast to previous studies[3,4] which investigated the PK of the ATX parent compound alone, the study presented herein developed a more comprehensive model by simultaneously fitting plasma and urine PK data collected for ATX and four different metabolites, which provided more mechanistic insights on ATX dispositions. Although the use of weight-based ATX dosing reduced the impact of body weight on the steady-state ATX exposures (e.g., AUC_{ss}), the significant impact of CYP2D6 AS on ATX AUC_{ss} was retained (**Figure 4b**), suggesting the need for initial ATX dose selection according to subjects' CYP2D6 phenotype, and subsequent dose adjustment over time as weight increases with age.

The ATX and 4-OH exposures were simulated and compared using the developed ATX PK model in subjects with various CYP2D6 phenotypes according to the ATX product label.[9] The current ATX product label recommends ATX dosing of 0.5 mg/kg q.d. in subjects with body weight <70 kg, regardless of CYP2D6 phenotype, and gradually titrated to 1.2 mg/kg q.d. with the

maximum total daily ATX dose of 1.4 mg/kg.[9] In this analysis, the ATX C_{max} and AUC_{0-24} at 9th dosing day (approximate steady-state) were used as the primary metrics for assessing the exposure to achieve therapeutic effects. Interestingly, our simulations suggested that the majority of subjects with a CYP2D6 AS of 1–3 cannot achieve a 400 ng/mL steady-state C_{max} at 0.5 mg/kg q.d. dosing, although the majority of subjects with an CYP2D6 AS < 1 could reach this concentration. This indicates that a higher dose of ATX might be needed for subjects with CYP2D6 AS of 1–3 as compared with subjects with CYP2D6 AS of < 1. To match the steady-state ATX C_{max} following a 0.5 mg/kg q.d. dose of ATX in AS 0 subjects, CYP2D6 AS 1–3 subjects would need an ~ 1.2 mg/kg q.d. dose (**Figure 5a**). These results were generally consistent with the dosing recommendations suggested by the ATX/CYP2D6 CPIC guideline.[12,28] Although both the ATX and unconjugated 4-OH are pharmacologically active, the concentration range of ATX is ~ 100-fold higher than the unconjugated 4-OH (**Figure 2**). *In vitro* studies suggested the affinity of 4-OH to the presynaptic norepinephrine transporters (the main pharmacological target) is similar to ATX, although the affinity to human serotonin transporter is higher for 4-OH than for ATX.[1,32] Although 4-OH exposures might not be as important as ATX exposures, one of the advantages of our model is the ability to simulate not only ATX parent compound exposures, but also ATX active metabolite exposures (i.e., 4-OH, **Figure 5b,d**), which potentially provides a valuable tool for future more comprehensive investigations of the ATX dose-exposure-response relationship involving both parent compound (ATX) and active metabolite (4-OH).

The model developed in this study could serve as a promising tool to explore various relevant clinical ATX questions. Here, we just provided two examples in terms of the plausible applications: (1) because our model incorporated CYP2D6 AS as a covariate, our model might be useful to explore the inter-individual variability contributions from CYP2D6 and non-CYP2D6 factors, and (2) our model may also be useful to explore dose adjustments in pediatric patients as they grow by leveraging demographic information from publicly available database, such as National Health and Nutrition Examination Survey (NHANES).[33]

The limitations of our analysis are noted. First, the model developed herein assumed ATX is only eliminated through 4-OH, NDA, and 2-COOH (2-methyl-OH)-mediated metabolism, and urinary excretion as unchanged ATX, without the consideration of other minor elimination pathways. Second, the developed model did not include the pharmacodynamic (PD) components. Thus, all the dose related simulations are based entirely upon the comparison of certain exposure metrics (e.g., ATX C_{max} and AUC_{0-24} at day 9). Future studies involving comprehensive exposure-response (ER) analysis will provide a clearer guidance of exposure matching simulations to inform clinical dosing of ATX based on this model. Nevertheless, the final ATX model was translated in an open-source platform and was provided in the supplementary material, along with a concise user guide (**Supplementary material: ATX-mrgsolve-model-guide.pdf**). This will allow the easy use of this model to inform the future clinical ATX dose exploration once additional ATX ER research becomes available. Additionally, it is noted that the study presented herein extrapolated the steady-state drug exposures using a model developed from single dose ATX PK data, which may warrant further validation once future steady state ATX PK data become available. However, considering the linear nature of ATX PKs,[4,9] the extrapolation into steady-state ATX PK performed using the model presented herein should be of low risk.

In conclusion, the study presented herein developed a comprehensive PK model to characterize the PK profiles of ATX and its metabolites in both plasma and urine, with the inclusion of CYP2D6 AS and body weight effects on model parameters. The developed ATX PK model is anticipated to be used in the future dose exploration of ATX with the appropriate integration of a PK-PD/ER framework.

SUPPORTING INFORMATION

Supplementary information accompanies this paper on the *Clinical Pharmacology & Therapeutics* website (www.cpt-journal.com).

FUNDING

The raw data generated for this study was supported through grant 1R01 HD058556 from the National Institutes of Health's Eunice Kennedy Shriver National Institute of Child Health and Human Development (Leeder, co-PI).

CONFLICT OF INTEREST

The authors declared no competing interests for this work.

AUTHOR CONTRIBUTIONS

S.C., M.A., J.S.L., and J.T.B. wrote the manuscript. S.C., M.A., J.S.L., and J.T.B. designed the research. S.C. and M.A. performed the research. S.C., M.A., J.S.L., and J.T.B. analyzed the data.

1. Sauer, J.M., Ring, B.J. & Witcher, J.W. Clinical pharmacokinetics of atomoxetine. *Clin. Pharmacokinet.* **44**, 571–590 (2005).
2. Ring, B.J., Gillespie, J.S., Eckstein, J.A. & Wrighton, S.A. Identification of the human cytochromes P450 responsible for atomoxetine metabolism. *Drug Metab. Dispos.* **30**, 319–323 (2002).
3. Sauer, J.M. *et al*. Disposition and metabolic fate of atomoxetine hydrochloride: the role of CYP2D6 in human disposition and metabolism. *Drug Metab. Dispos.* **31**, 98–107 (2003).
4. Witcher, J.W. *et al*. Atomoxetine pharmacokinetics in children and adolescents with attention deficit hyperactivity disorder. *J. Child Adolesc. Psychopharmacol.* **13**, 53–63 (2003).
5. Brown, J.T., Abdel-Rahman, S.M., van Haandel, L., Gaedigk, A., Lin, Y.S. & Leeder, J.S. Single dose, CYP2D6 genotype-stratified pharmacokinetic study of atomoxetine in children with ADHD. *Clin. Pharmacol. Ther.* **99**, 642–650 (2016).
6. Gaedigk, A., Simon, S.D., Pearce, R.E., Bradford, L.D., Kennedy, M.J. & Leeder, J.S. The CYP2D6 activity score: translating genotype information into a qualitative measure of phenotype. *Clin. Pharmacol. Ther.* **83**, 234–242 (2008).
7. Yu, G., Li, G.F. & Markowitz, J.S. Atomoxetine: a review of its pharmacokinetics and pharmacogenomics relative to drug disposition. *J. Child Adolesc. Psychopharmacol.* **26**, 314–326 (2016).
8. de Leon, J. Translating pharmacogenetics to clinical practice: do cytochrome P450 2D6 Ultrarapid metabolizers need higher

atomoxetine doses? *J. Am. Acad. Child Adolesc. Psychiatry* **54**, 532–534 (2015).
9. *Strattera (atomoxetine hydrochloride) capsules label*. [cited 2023 Oct. 26th]; <https://www.accessdata.fda.gov/drugsatfda_docs/label/2011/021411s035lbl.pdf>.
10. ter Laak, M.A. *et al*. Recognition of impaired atomoxetine metabolism because of low CYP2D6 activity. *Pediatr. Neurol.* **43**, 159–162 (2010).
11. de Leon, J. The crucial role of the therapeutic window in understanding the clinical relevance of the poor versus the ultrarapid metabolizer phenotypes in subjects taking drugs metabolized by CYP2D6 or CYP2C19. *J. Clin. Psychopharmacol.* **27**, 241–245 (2007).
12. Brown, J.T. *et al*. Clinical pharmacogenetics implementation consortium guideline for cytochrome P450 (CYP)2D6 genotype and atomoxetine therapy. *Clin. Pharmacol. Ther.* **106**, 94–102 (2019).
13. Gaedigk, A., Bradford, L.D.A., Alander, S.W. & Leeder, J.S. CYP2D6*36 gene arrangements within the cyp2d6 locus: association of CYP2D6*36 with poor metabolizer status. *Drug Metab. Dispos.* **34**, 563–569 (2006).
14. Gaedigk, A., Fuhr, U., Johnson, C., Bérard, A., Bradford, L.D.A. & Leeder, J.S. CYP2D7-2D6 hybrid tandems: identification of novel CYP2D6 duplication arrangements and implications for phenotype prediction. *Pharmacogenomics* **11**, 43–53 (2010).
15. Gaedigk, A. *et al*. Identification of novel CYP2D7-2D6 hybrids: non-functional and functional variants. *Front. Pharmacol.* **1**, 121 (2010).
16. Gaedigk, A. *et al*. Cytochrome P4502D6 (CYP2D6) gene locus heterogeneity: characterization of gene duplication events. *Clin. Pharmacol. Ther.* **81**, 242–251 (2007).
17. Dinh, J.C., Pearce, R.E., van Haandel, L., Gaedigk, A. & Leeder, J.S. Characterization of atomoxetine biotransformation and implications for development of PBPK models for dose individualization in children. *Drug Metab. Dispos.* **44**, 1070–1079 (2016).
18. Boeckmann, A.J., Sheiner, L.B. & Beal, S.L. *NONMEM Users Guide - Part V* (ICON Plc NONMEM Project Group, Gaithersburg, MD: Gaithersburg, Maryland and University of California at San Francisco, San Francisco, CA 2017).
19. Kay, K. *et al*. *A Suite of Open-Source Tools to Guide Efficient Pharmacometric Analyses*, in *American Conference on Pharmacometrics (ACOP)* (2022) Denver.
20. Savic, R.M. & Karlsson, M.O. Importance of shrinkage in empirical bayes estimates for diagnostics: problems and solutions. *AAPS J.* **11**, 558–569 (2009).
21. Nguyen, T.H. *et al*. Model evaluation of continuous data Pharmacometric models: metrics and graphics. *CPT Pharmacometrics Syst. Pharmacol.* **6**, 87–109 (2017).
22. Dosne, A.G., Bergstrand, M., Harling, K. & Karlsson, M.O. Improving the estimation of parameter uncertainty distributions in nonlinear mixed effects models using sampling importance resampling. *J. Pharmacokinet. Pharmacodyn.* **43**, 583–596 (2016).
23. Dosne, A.G., Bergstrand, M. & Karlsson, M.O. An automated sampling importance resampling procedure for estimating parameter uncertainty. *J. Pharmacokinet. Pharmacodyn.* **44**, 509–520 (2017).
24. Bergstrand, M., Hooker, A.C., Wallin, J.E. & Karlsson, M.O. Prediction-corrected visual predictive checks for diagnosing nonlinear mixed-effects models. *AAPS J.* **13**, 143–151 (2011).
25. Kane, M. In *CYP2D6 Overview: Allele and Phenotype Frequencies, in Medical Genetics Summaries [Internet]* (eds. Pratt, V.M., Pirmohamed, M. *et al*.) (National Center for Biotechnology Information (US), Bethesda (MD), 2021).
26. Baron, K.T. *mrgsolve* [cited 2023 04/24]; <https://mrgsolve.org/>.
27. Baron, K.T. *Validate model translation from NONMEM* (2022) [cited 2023 03/21]; <https://mrgsolve.org/blog/posts/2022-05-validate-translation/>.
28. Michelson, D. *et al*. CYP2D6 and clinical response to atomoxetine in children and adolescents with ADHD. *J. Am. Acad. Child Adolesc. Psychiatry* **46**, 242–251 (2007).
29. Huang, Y. *et al*. Deciphering genetic causes for sex differences in human health through drug metabolism and transporter genes. *Nat. Commun.* **14**, 175 (2023).
30. Cheng, S., Flora, D.R., Rettie, A.E., Brundage, R.C. & Tracy, T.S. Pharmacokinetic modeling of warfarin capital I, Ukrainian—model-based analysis of warfarin enantiomers with a target mediated drug disposition model reveals CYP2C9 genotype-dependent drug-drug interactions of S-warfarin. *Drug Metab. Dispos.* **50**, 1287–1301 (2022).
31. Cheng, S., Flora, D.R., Rettie, A.E., Brundage, R.C. & Tracy, T.S. Pharmacokinetic modeling of warfarin capital I, Ukrainianl—model-based analysis of warfarin metabolites following warfarin administered either alone or together with fluconazole or rifampin. *Drug Metab. Dispos.* **50**, 1302–1311 (2022).
32. Wong, D.T., Threlkeld, P.G., Best, K.L. & Bymaster, F.P. A new inhibitor of norepinephrine uptake devoid of affinity for receptors in rat brain. *J. Pharmacol. Exp. Ther.* **222**, 61–65 (1982).
33. *National Health and Nutrition Examination Survey*. [cited 2023 Jul. 4th]; <https://www.cdc.gov/nchs/nhanes/index.htm>.